Three Methods for Event-Type Identification in the SNO Detector SNO-STR-95-002

T. J. Radcliffe
Dept. of Physics
Queen's University at Kingston
Ontario CANADA K7L 3N6

January 17, 1995

1 Introduction

This report follows SNO-STR-94-019[1]. Further work with the circular Hough Transform (CHT) is described, as well as two other methods for distinguishing CC from NC (that is, Cl-capture) events on a statistical basis. These are: maximum likelihood in energy and angle, and average nearest neighbour distance (ANND). Both of the latter methods appear to work somewhat better than the CHT, giving us three essentially independent methods of determining the number of NC events without having to subtract salt-out runs from salt-in runs. Each of these methods may be used to extract 30 to 40 % of the NC events on an event-by-event basis with relatively small contamination by CC events.

The ideal event-type identification parameter would have the following properties:

- Clean separation of NC and CC events
- Independent of details of MC
- Independent of nhit

Visual inspection of CC and NC events strongly suggests that the first property is not achievable. Figure 1 shows a selection of CC and NC events, and the reader is encouraged to try to lump them into two groups prior to reading the key appended to this paper. The second property is perhaps the most important: we want to be very sure that we are not developing algorithms that are sensitive to properties of the MC rather that properties of the detector. The three parameters discussed here are expected to have varying levels of sensitivity to MC parameters: the CHT should be sensitive only to the number of PMTs in the best ring and not the overall angular distribution, the likelihood should be sensitive to the average angular distribution at a given energy but not to the fine details like the ring patterns, and ANND should be sensitive only to the crudest aspects of the angular distribution. The only instance that might result in none of these parameters being effective on the real data is if both CC and NC events appear as undifferentiated isotropic blobs, and events published by Kamiokande suggest that this will not be the case.

The final property of nhit independence is desirable but not necessary: it is always possible to do a channel-by-channel analysis, so only events of the same nhit are being compared. Note that to do any of the comparisons described in this report it will almost certainly be necessary to have the ^{8}Li source available to generate pattern-calibration data for a pure electron spectrum. Preliminary comparisons indicate that while the differences between γ-rays and electrons are too small to be useful, they are large enough to prevent γs from being used to calibrate pattern recognition algorithms.

All tests described here were performed using a data set generated by the calibration Monte Carlo. This was done because it was at the time the only code available that corrected for the direction of the electron prior to the emission of every Cherenkov photon. EGS4 uses a straight transport step and corrects the direction of the electron for multiple scattering at the end of the step. The lateral displacement of the electron is not corrected for, as this would make geometric calculations prohibitively difficult. This problem is fairly small at high energies, but NC events include lower-energy photons, so it was thought useful to do a simple correction. The electron is turned linearly as it moves along the straight step according to:

$$\hat{u}(t) = \hat{u}_i + (\hat{u}_f - \hat{u}_i) \times t \qquad (1)$$

where

$$\begin{aligned} \hat{u}_i &= \text{initial electron direction} \\ \hat{u}_f &= \text{final electron direction} \\ t &= \text{fractional step length (varies between 0 and 1)} \end{aligned}$$

The spectra for NC and CC events are shown in Figure 2. 5.5 MeV electrons where used as CC events because they produced the same nhit spectrum and for the purposes of comparison it was desired to remove any nhit-dependence from the comparisons. In both cases 1000 events uniformly distributed throughout the acrylic vessel were used, and in the analysis only events that reconstructed inside 550 cm were used. This meant that only about 750 events were used in the analysis, as $\sim$ 23 % of the volume was excluded from the analysis. All fitting was performed with the modal fitter. The time resolution of the PMTs was taken to be 1.6 ns and the noise rate per PMT 1000 Hz. The NC spectrum used was essentially identical to that used in QMC: this spectrum is a simple approximation involving only a few branches, and it is expected that the correct spectrum will result in even more diffuse patterns than the approximate one. Further work with SNOMAN will be done to check this.

2 Projection of Events

Previous work on the CHT involved projecting events onto a plane normal to the reconstructed direction. Ira Blevis has suggested a much better way of projecting events, in which the planar co-ordinates (x, y) are given by:

$$\begin{aligned} x &= \theta \times \cos\phi \\ y &= \theta \times \sin\phi \end{aligned}$$

where θ is the angle relative to the reconstructed direction and ϕ is the azimuthal angle relative to the plane containing the z-axis and the event direction. If the event direction was along the z-axis the azimuthal angle was taken relative to the x-axis.

When the reconstructed direction corresponds to the event direction the Cherenkov cone produced while the electron was traveling in the initial direction forms a circular ring of radius 41 degrees in the plane of projection. If the reconstructed direction is incorrect this ring is off-centre and elliptical.

3 Circular Hough Transform

A single-ring CHT was used, rather than the concentric weighted ring CHT described previously[1][2]. The results with a single ring are as good as those with concentric weighted rings, and using a single ring means the algorithm is sensitive only to the number of PMTs in the best ring, not to the overall angular distribution. The plane of projection was divided into 81 $\times$ 81 pixels, so each pixel is 4.4 $\times$ 4.4 degrees. A 3 $\times$ 3 pixel region is averaged to find the best circle, and the event direction is corrected to move this peak to the centre of the plane of projection. After directional correction, the fraction of hits in the best circle is given by the fraction of hits in the central pixel of the plane of projection. All of these calculations are performed for hits whose time residuals are less than $\pm 3\ \sigma = \pm 4.8$ ns; scattered light is eliminated from the calculation.

The results can be seen in Figure 3. The peaks are approximately Gaussian and separated by slightly less than 1σ. This is not quite as good as the separation achieved using QMC events, and may reflect the significance of the decreased correlation due to correcting the electron direction along the step. Previous work indicates it will be possible to use the parameter at this level of separation to extract the fraction of CC and NC events with about twice the statistical error.

4 Likelihood in Energy and Angle

Figure 4 shows the angular distribution as a function of energy for the EGS4 parameter ESTEPE set to 0.01. This angular distribution can be used to generate a likelihood that includes all of the information about the event as follows (note: I didn't really intend to investigate this technique, but the algorithm just fell out of work I was doing on optical correction, so I thought I'd include it here for comparison with similar work being done by Josh Klein

at Penn.)

For an electron at time t with position $\vec{x}$, initial direction $\hat{u}$ and energy E the mean number of Cherenkov photons emitted into the solid angle of PMT i is:

$$N_e^i = \left[\frac{dN}{d\cos\theta}\right] \frac{r^2(-\hat{u}_p \cdot \hat{u}_i)}{2R^2} \tag{2}$$

where

$$\begin{aligned}
\frac{dN}{d\cos\theta} &= \text{angular distribution of emitted photons} \\
\theta &= \text{angle between emitted photon and electron direction} \\
R &= |\vec{x}_i - \vec{x}|\text{(distance from event position to PMT } i\text{)} \\
\vec{x}_i &= \text{position of PMT } i \\
\hat{u}_p &= \frac{\vec{x}_i - \vec{x}}{R}\text{(direction of optical photon)} \\
\hat{u}_i &= \text{inward direction of PMT} \\
r &= \text{radius of the PMT/concentrator face}
\end{aligned}$$

The angular distribution of photons from the electron, $\frac{dN}{d\cos\theta}$, is a function of energy as well as angle: it is the number of photons emitted between $\cos(\theta - d\theta)$ and $\cos(\theta + d\theta)$ (where $d\theta$ is the half-angle subtended by the PMT) for an electron of energy E.

The number of photons detected by the PMT depends on the absorption probabilities in the D_2O , the acrylic and the H_2O , as well as on the reflection probabilities at the water/acrylic interfaces and on the PMT quantum efficiency. Nominally, the probability of PMT i detecting a photon emitted toward it is:

$$P_d^i = \epsilon^i(l_{D_2O}, l_{acr}, l_{H_2O}) \times P_s \times (1 - P_{ri}) \times (1 - P_{ro}) \times \mathcal{R}(\hat{u}_p \cdot \hat{u}_i) \tag{3}$$

where

$$\epsilon(l_{D_2O}, l_{acr}, l_{H_2O}) = \text{effective QE of PMT}$$

$$
\begin{aligned}
P_s &= exp(-l_{D_2O}/\lambda_{D_2O} - l_{acr}/\lambda_{acr} - l_{H_2O}/\lambda_{H_2O}) \\
&= \text{survival probability through optical media} \\
P_{ri} &= \text{reflection probability at inner acrylic surface} \\
P_{ro} &= \text{reflection probability at outer acrylic surface} \\
\mathcal{R}(\hat{u}_p \cdot \hat{u}_i) &= \text{angular response of PMT/concentrator} \\
&\quad \text{combination } \textit{not including solid angle}
\end{aligned}
$$

The l's are the photon path length in each medium and the λ's are the absorption length in each medium. The relation for the survival probability is true for any single wavelength, but because the spectral shape changes significantly over the path length of the light it is not possible to define a single absorption length for Cherenkov light in the SNO detector. The effective absorption length for acrylic, for instance, is about 12 cm for a 5 cm thick sheet and 18 cm for a 10 cm thick sheet, purely because of spectral shape changes. It is therefore necessary to determine the actual survival probability of any photon by integrating the absorption over the spectral shape. The same is true of the quantum efficiency, which is why it is shown as depending on the path length through each medium. Note that the lengths in each medium have to be corrected for refraction at the acrylic surfaces: this is the most tedious part of the calculation, and makes performing the sum over all PMTs extremely slow, taking several minutes per event.

Multiplying the mean number of photons emitted in the direction of PMT i by the detection probability gives the mean number of photons detected by that PMT for the assumed event parameters:

$$N_d^i = P_d^i \times N_e^i \tag{4}$$

This value is used to calculate a log-likelihood for the event parameters according to:

$$L = -\sum_{j=unhit} \ln(\exp(-N_d^j)) - \sum_{k=hit} \ln((1 - \exp(-N_d^k)) \times 0.9973) \tag{5}$$

where the factor 0.9973 accounts for the 3σ limits put on in-time light by the modal fitter (it is also possible to weight individual photons by a normalized Gaussian with a mean of zero and standard deviation of 1.6 ns to

account for the arrival-time residual *dt* for each PMT, but as the modal fitter forces the arrival-time distribution to have this shape in any case, doing this adds no further information to the likelihood.)

The sums are over hit and unhit PMTs, so the likelihood is the joint probability of all PMTs that are not hit of not getting hit, and all the PMTs that are hit of getting hit. Calculating the likelihood in this way includes all the available information about the event with the important exception that scattered and reflected light is treated as "undetected". Note that for hit PMTs a minimum probability is artificially imposed on the algorithm, given by the noise rate: scattered or reflected photons that result in very low hit probabilities are assigned the probability arising from the noise rate and the $\pm$ 100 ns trigger window.

Figure 5 shows the difference between the log-likelihood calculated from the assumption that the event is NC and that calculated from the assumption that the event is CC for both NC and CC events. The NC assumption was incorporated by assuming an isotropic distribution of source photons. Recall that under the assumption an event is a NC event, the fitted direction is a meaningless artifact of the fitter and there is no particular direction that should be prefered over any other in the analysis. The angular distribution of NC photons relative to the first γ-ray in the event is almost flat, making isotropy a fairly good approximation. For the NC likelihood the number of photons was set equal to the mean number in a NC event. The peak at zero difference for NC events are events in which the NC assumption produced a greater likelihood than the CC assumption. For most NC events the difference between the best CC likelihood and the NC likelihood is smaller than the difference for CC events (that is, NC events are in fact more "NC-like" than CC events, even when a NC event appears more likely to be a CC event.)

Experience with the early CHT work suggests that the difference in the likelihood curves will be sufficient to allow good statistical extraction of the number of NC events from the mixed NC/CC spectrum, and the fraction of NC events that can be extracted with negligible CC contamination appears to be between 30 and 40 %. In short, this kind of maximum likelihood calculation appears a very promising way of determining the fraction of NC events in the salt-in SNO spectrum.

5 Event Diffuseness

Scanning events by hand one is struck by the relatively diffuse nature of NC hit patterns. Although there are many that are indistinguishable from CC hit patterns, there is a clear trend to more hits that are far away from all other hits. For this reason events were processed by calculating the average nearest neighbour distance (ANND) for in-time hits. The distance measure used was the Euclidean distance $\sqrt{(x_1 - x_2)^2 + (y_1 - y_2)^2}$ in the plane of projection.

The results for CC and NC events are shown in Figure 6. Although the peaks are not quite fully resolved, there is no question that this parameter can be used to distinguish NC and CC events on a statistical basis, and again about 35% of NC events can be extracted on an event-by-event basis with very little CC contamination.

6 Things That Don't Work So Well

As usual, quite a few parameters were investigated to find a few that seemed to work. Various subsets of hits were used to generate ANND parameters: hits on the best circle, all in-time hits except those on the best circle and all hits including those not in-time. None of these provided discrimination as good as ANND for all in-time hits, but they should be borne in mind when it comes to analyzing the real data.

Several parameters having to do with the distribution of hits on the best circle were investigated: in particular the average azimuthal angle between hits and the maximum gap in azimuthal angle on the circle. A little thought will show that the first of these parameters is closely related to the number of hits on the circle, and in fact it shows discrimination about equal to that of the CHT. The second is a slightly better measure of the "clumpy-ness" of the hits on the circle, and while NC events did tend to have slightly larger gaps in their best circles it was not really good enough to provide much discrimination.

7 Conclusion

Two new methods of distinguishing NC from CC events have been found that are sensitive to different parameters of hit distributions than the CHT algorithm. The likelihood method is sensitive only to the overall angular distribution, not the Cherenkov rings as such. ANND is sensitive to the diffuseness of the event, which while obviously not unrelated to the angular distribution in θ is not the same as it: two events with the same angular distribution in θ may have very different diffusenesses, depending on their ϕ distributions. The CHT as implemented for the work described here is sensitive only to the number of photons in the best ring, and not at all to the overall angular distribution.

All three algorithms appear to be able to distinguish CC and NC events at about the same level. Having three more-or-less independent means of distinguishing NC and CC events should add considerably to our confidence that we have done the job properly (or not) when it comes to analyzing the real data, and significantly increases the probability that we will not have to cycle the salt to extract the NC spectrum by subtraction. Furthermore, recall that by increasing the threshold on the analysis and watching the fraction of NC events drop, it is possible to extract the NC shape using any of these techniques. This means we not only have consistency between methods to act as a systematic check, but also for each method we can demand that the extracted NC shape be correct. This should make the extraction of the CC/NC ratio extremely robust against systematic errors in any one method.

An important feature that has been left out of this work is the background. Future work will include exploring the nhit-dependence and threshold-dependence of the parameters described here, as well as pursuing the promised investigation of single γ discrimination and PMT β/γ discrimination.

References

[1] T. J. Radcliffe, SNO-STR-94-019, Pattern Recognition for Event-Type Identification in the SNO Detector

[2] J. Illingworth and J. Kittler, A Survey of the Hough Transform, Computer Vision, Graphics and Image Processing 44 (1988) 87 - 116

A Key to events in Figure 1

NC events a,b,c,d,e

CC events f,g,h,i,j

B Figure Captions

Figure 1 Ten events projected in θ and ϕ. Half are NC, half are CC. A key is provided on the next page.

Figure 2 NC and CC spectra for events used to evaluate discrimination parameters.

Figure 3 CHT results for CC and NC events.

Figure 4 Angular distribution of photons from single electrons between 1 and 20 MeV for ESTEPE = 0.01 and electron directional correction.

Figure 5 Difference in log-likelihoods for NC and CC events analyzed under the assumptions of NC and CC events.

Figure 6 Average nearest-neighbour distance for NC and CC events. Distance is Euclidean distance in the plane of projection.

FIG. 1a

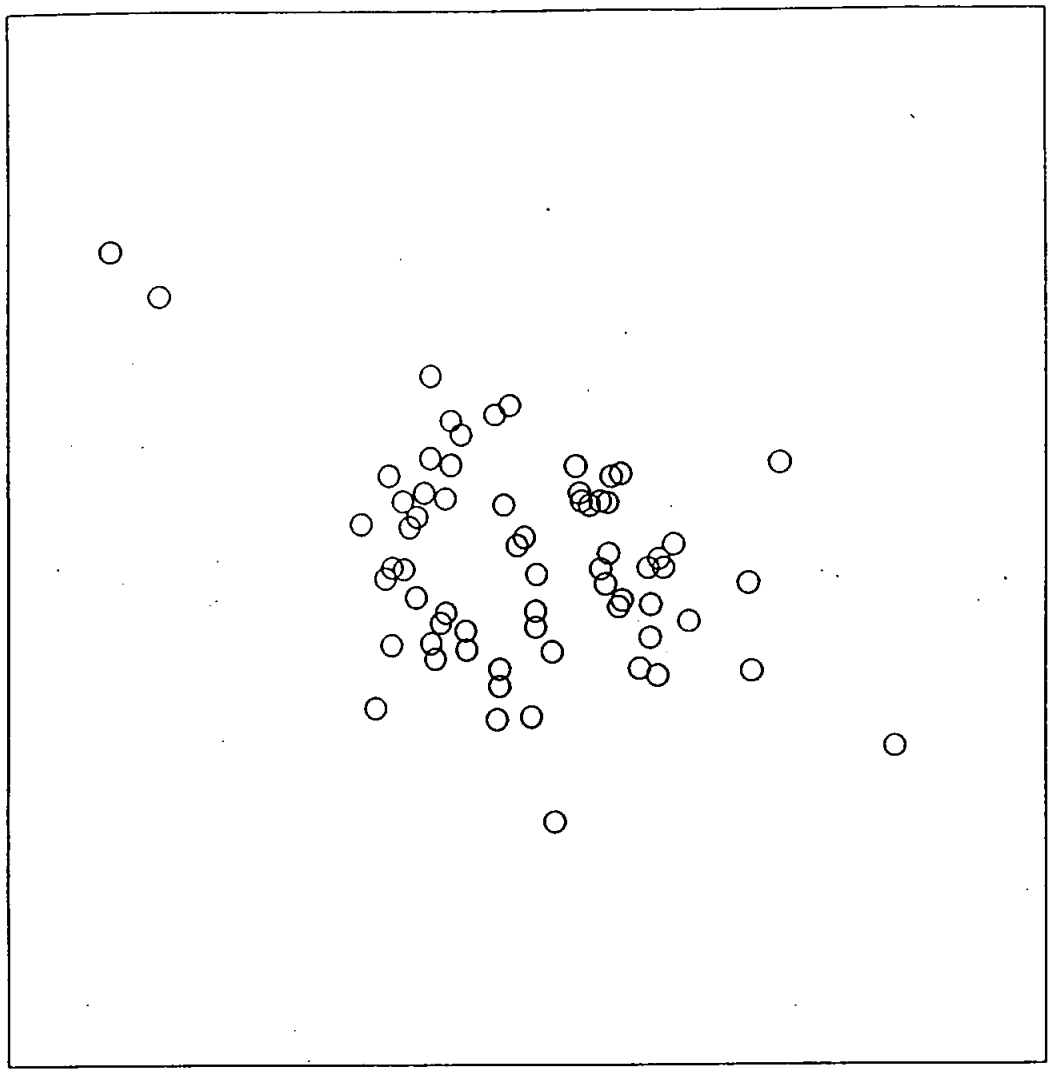

FIG: 1b

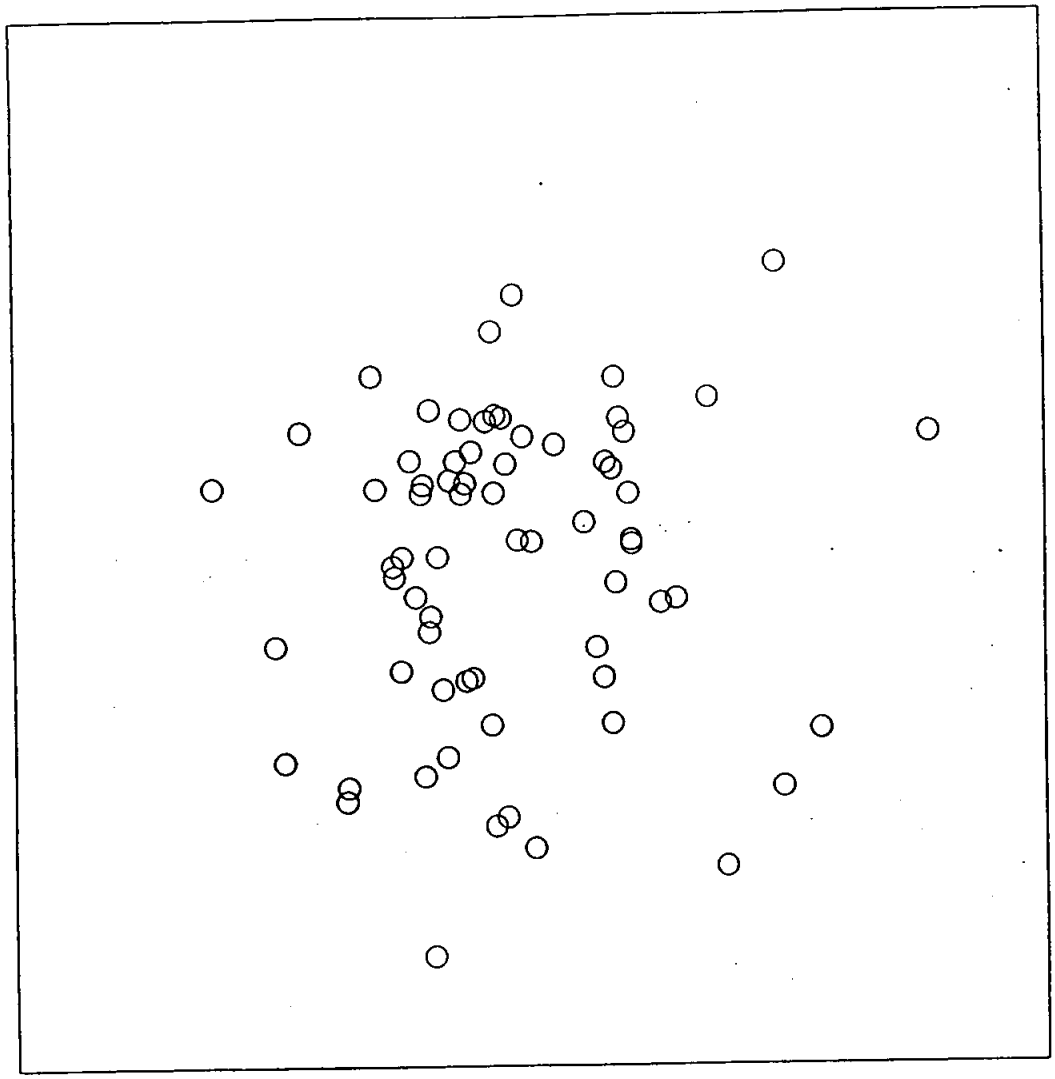

Fig. 1c

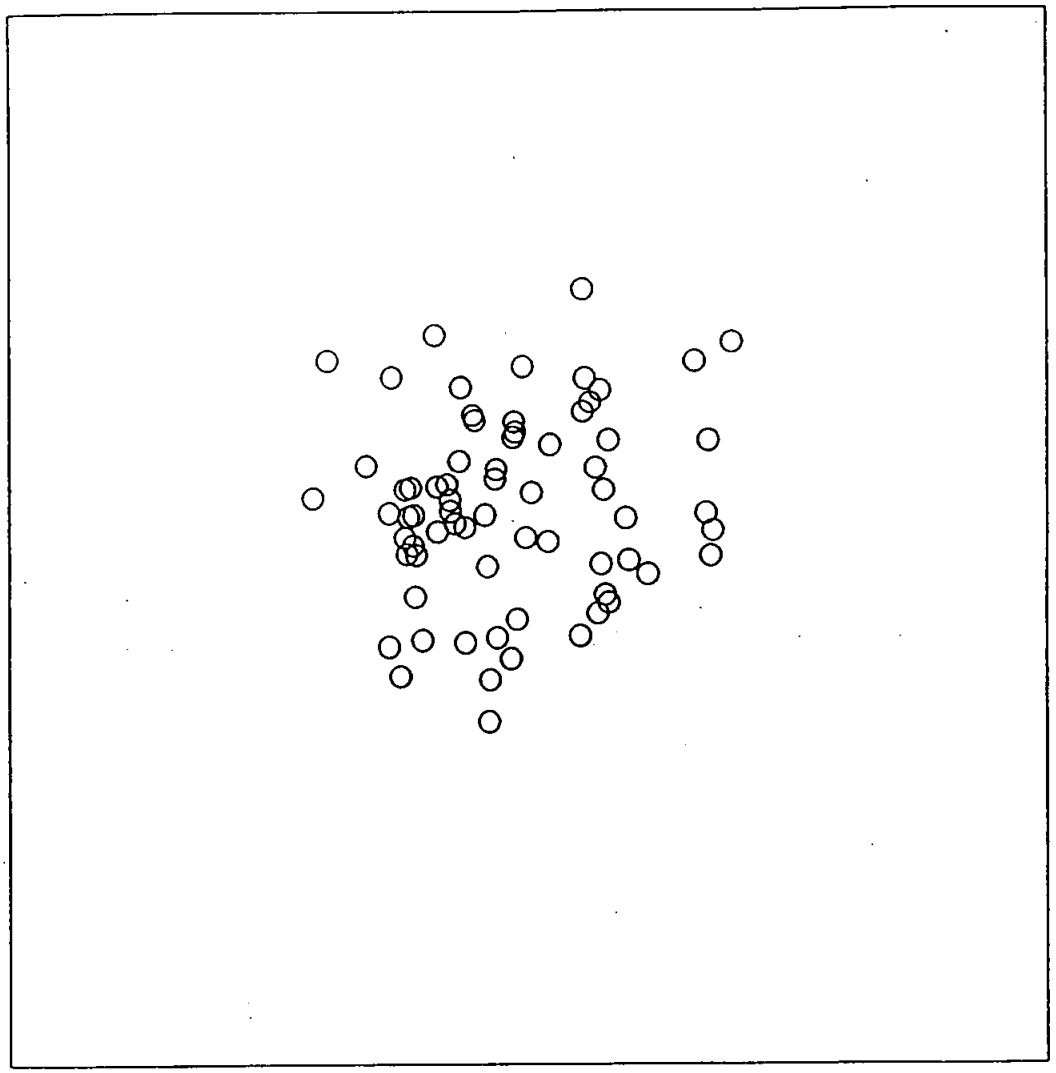

Fig. 1d

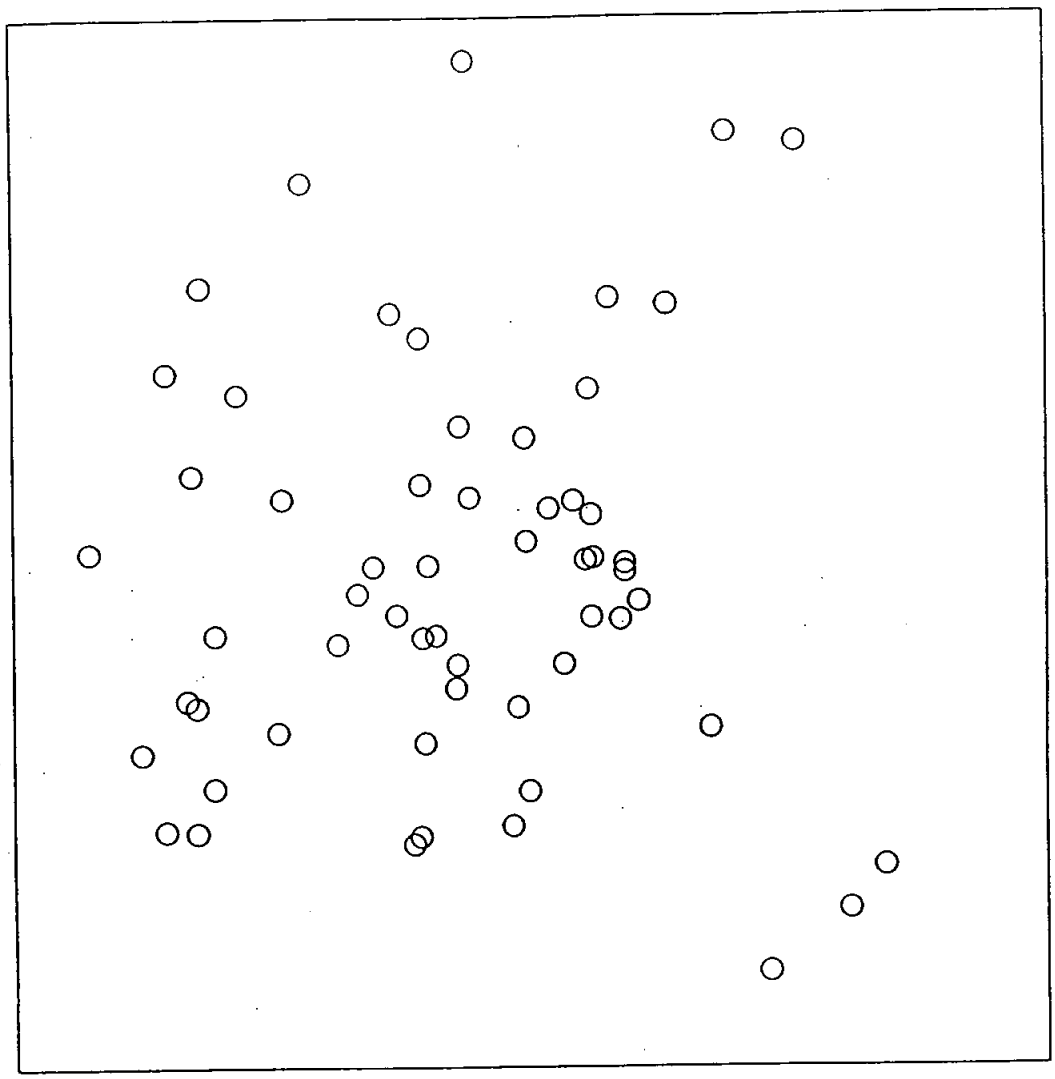

Fig. 1e

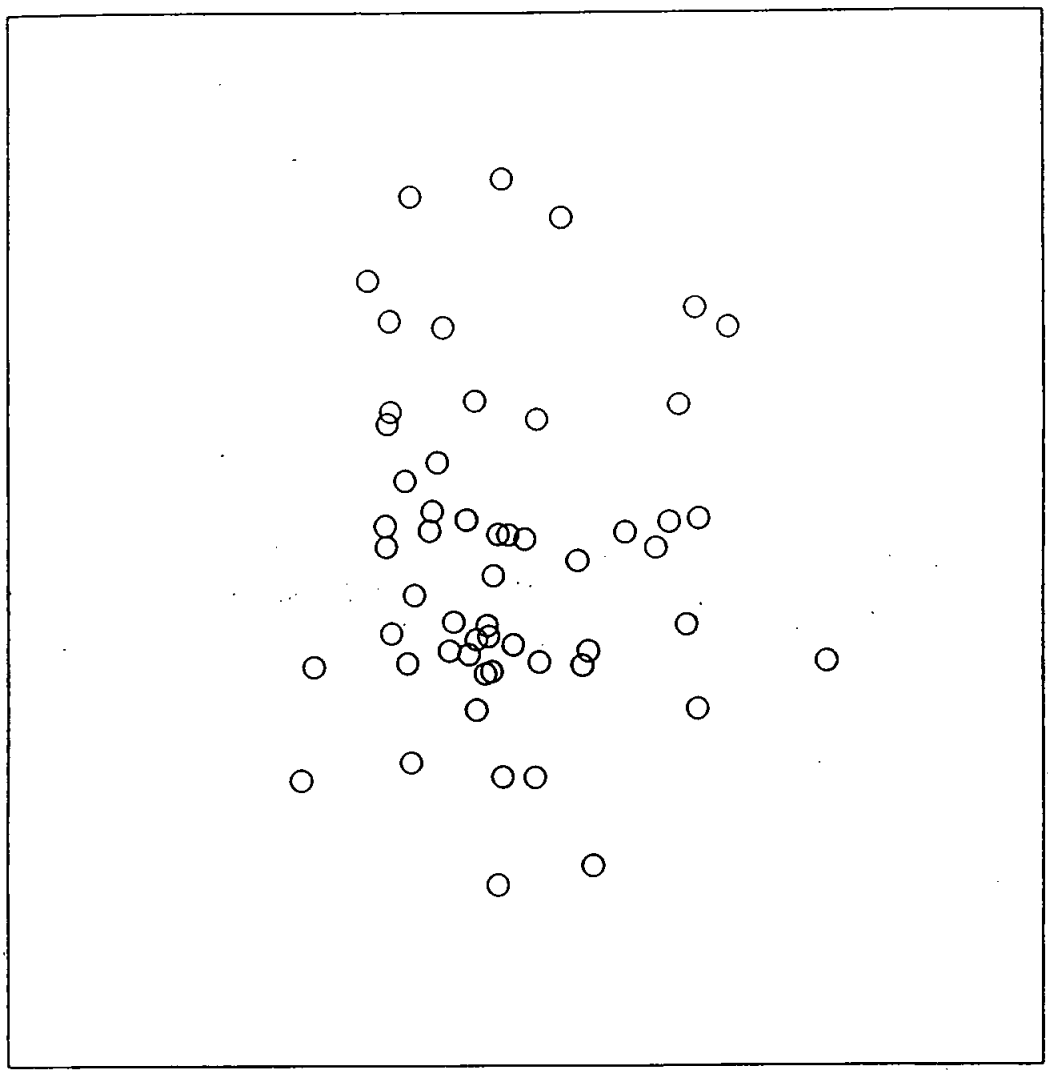

FIG. 1f

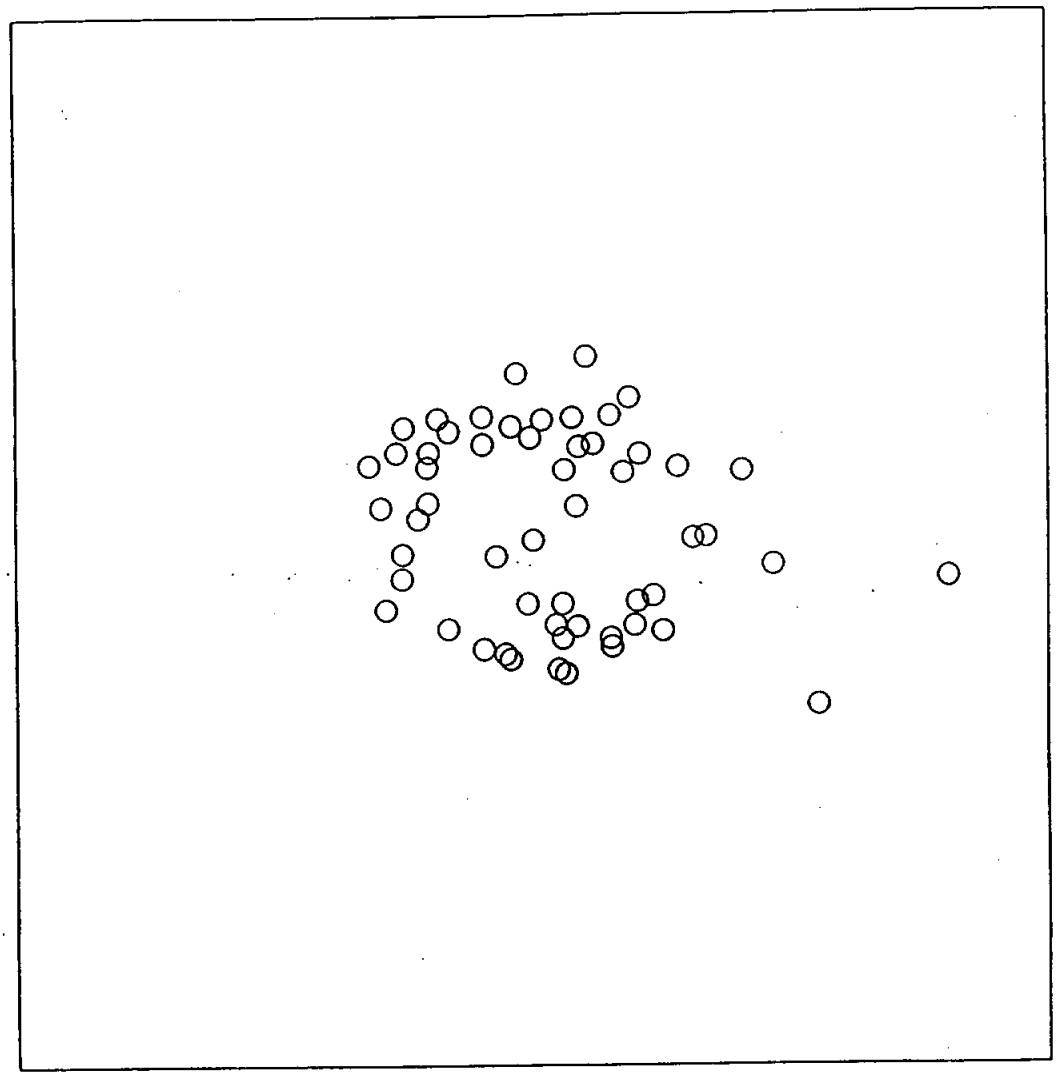

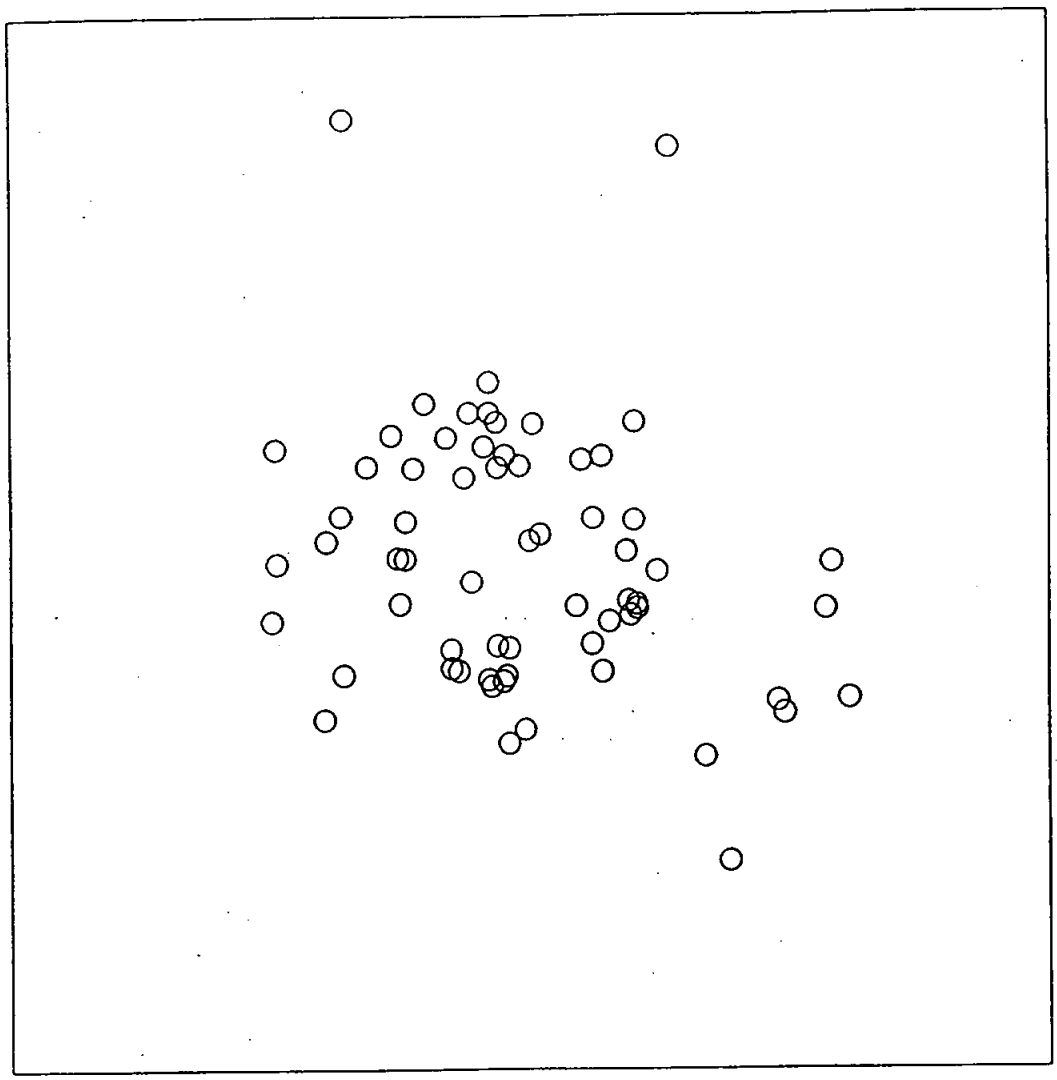

Fig. 1L

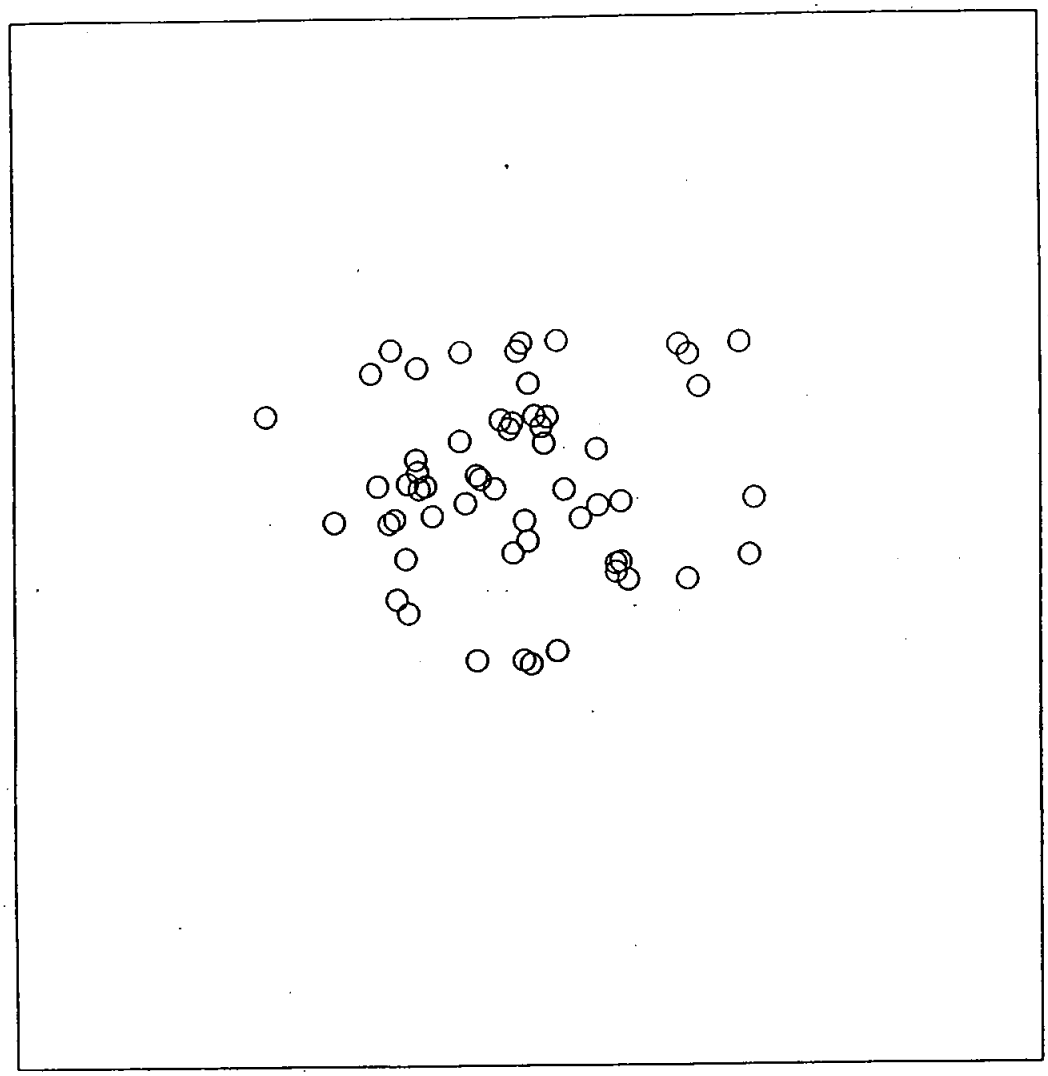

Fig. 1i

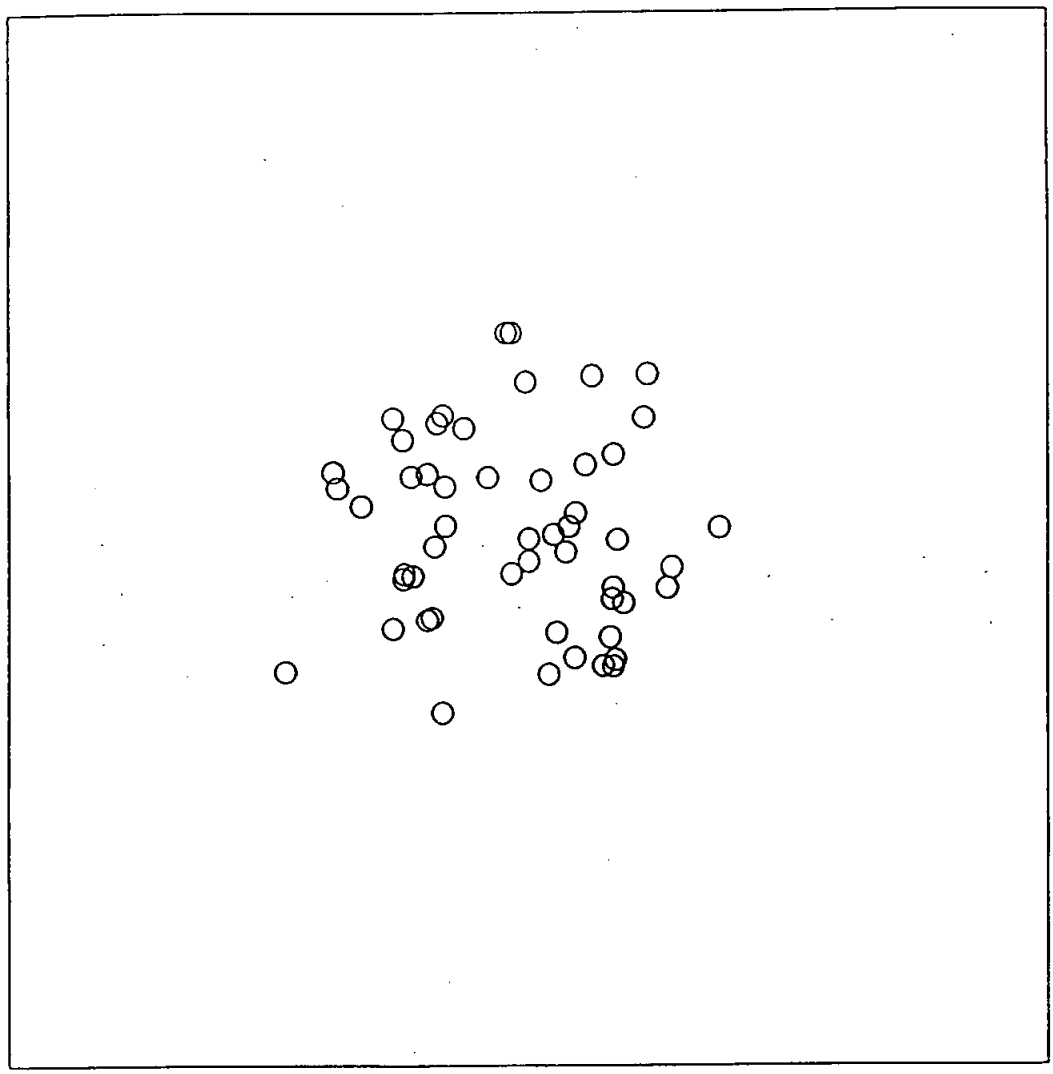

Fig. 1J

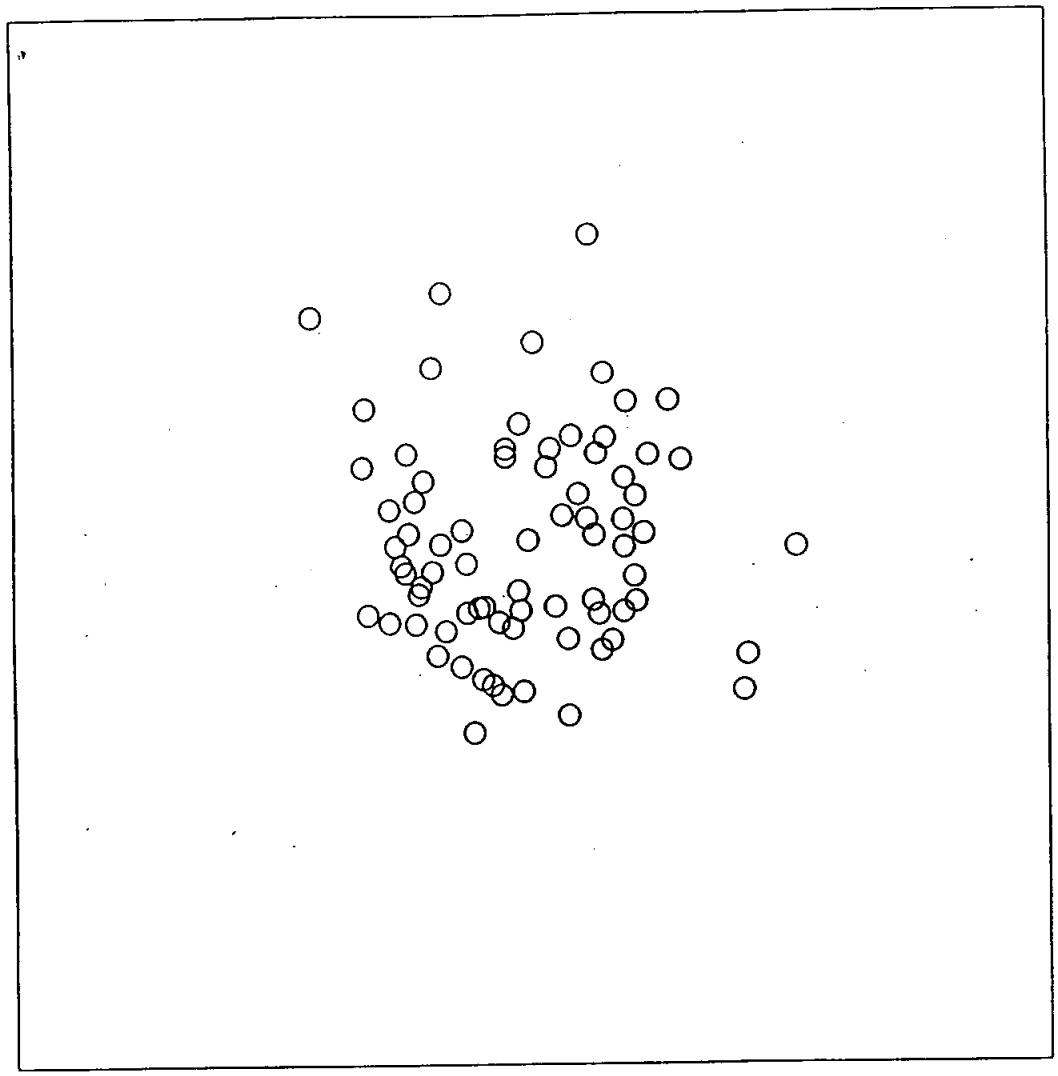

Fig. 2

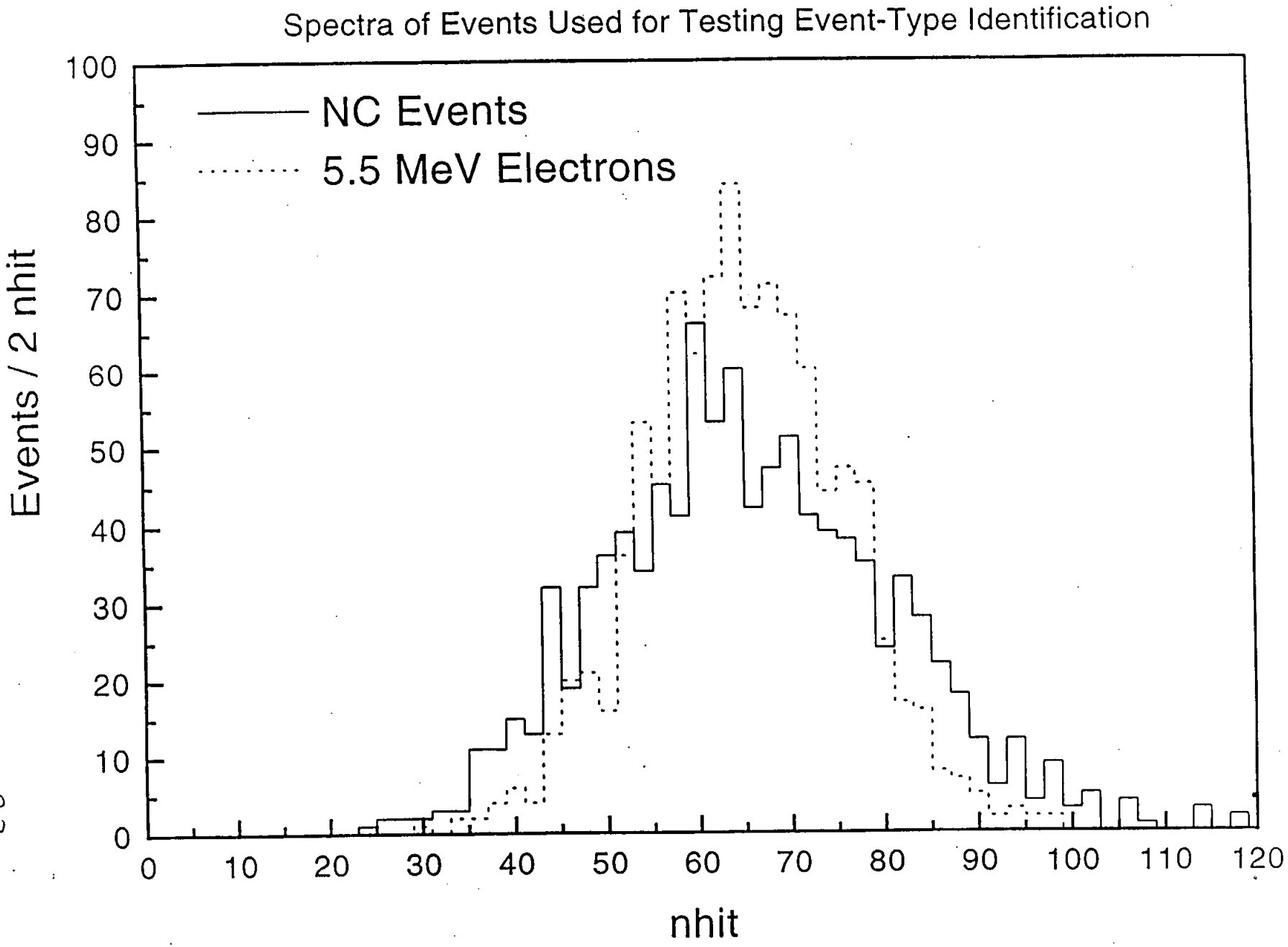
Spectra of Events Used for Testing Event-Type Identification
NC Events
5.5 MeV Electrons
Events / 2 nhit
nhit
0
10
20
30
40
50
60
70
80
90
100
110
120

Fig. 3

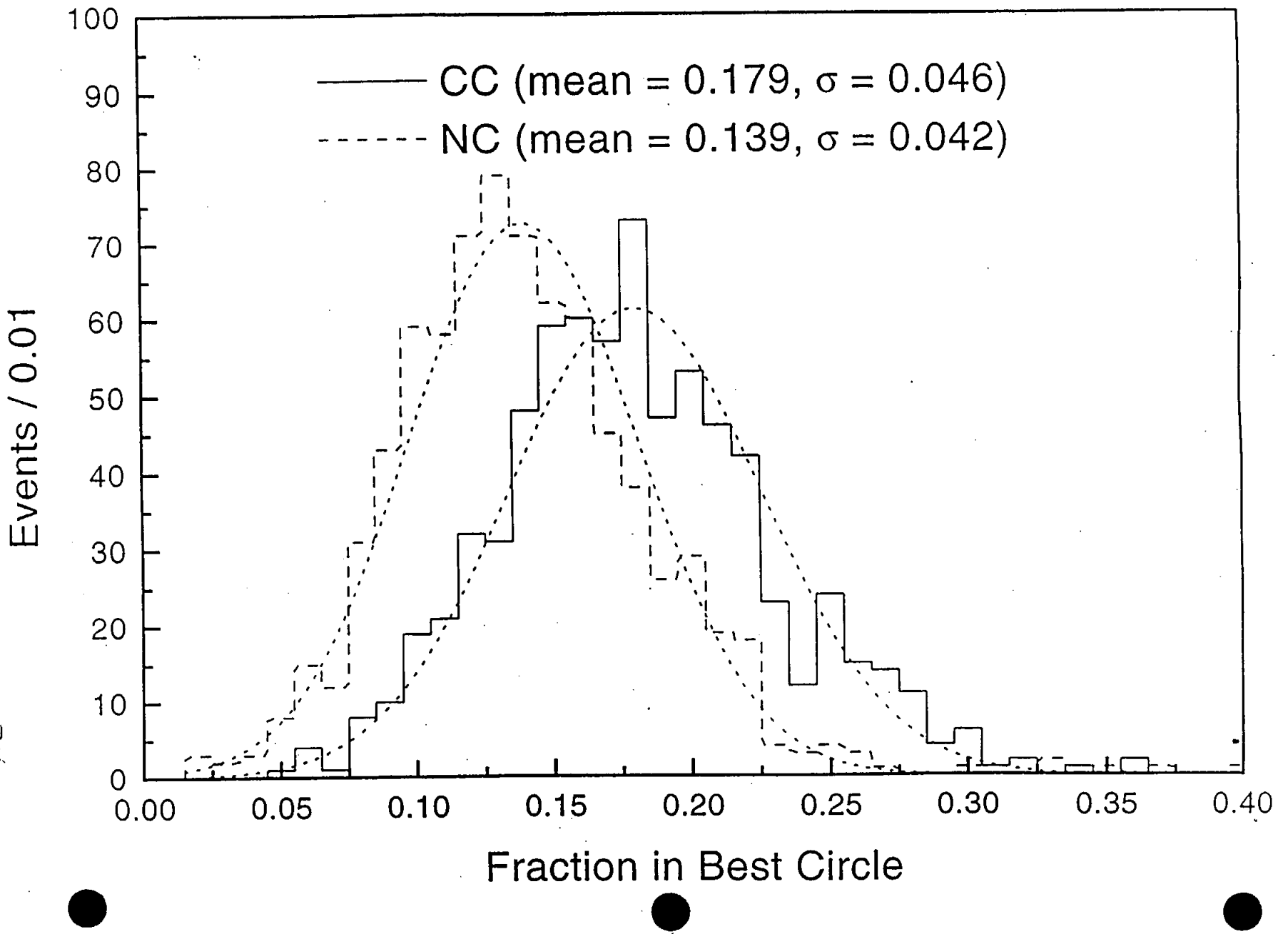
CC (mean = 0.179, σ = 0.046)
NC (mean = 0.139, σ = 0.042)
Events / 0.01
Fraction in Best Circle
0
10
20
30
40
50
60
70
80
90
100
0.00
0.05
0.10
0.15
0.20
0.25
0.30
0.35
0.40

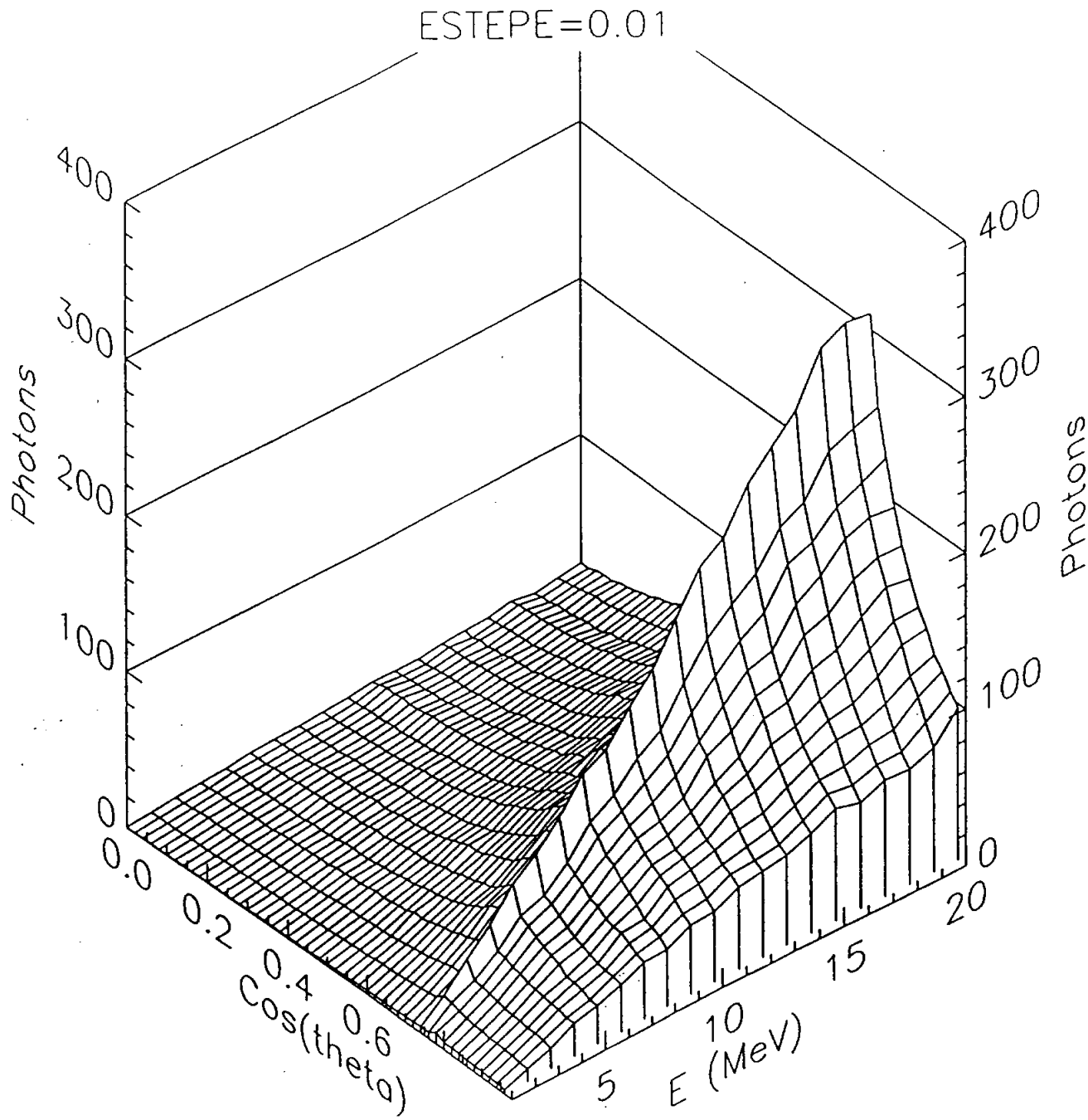
ESTEPE=0.01
Photons
400
300
200
100
0
0.0
0.2
0.4
0.6
Cos(theta)
5
10
15
20
E (MeV)

Fig. 4

Fig. 5

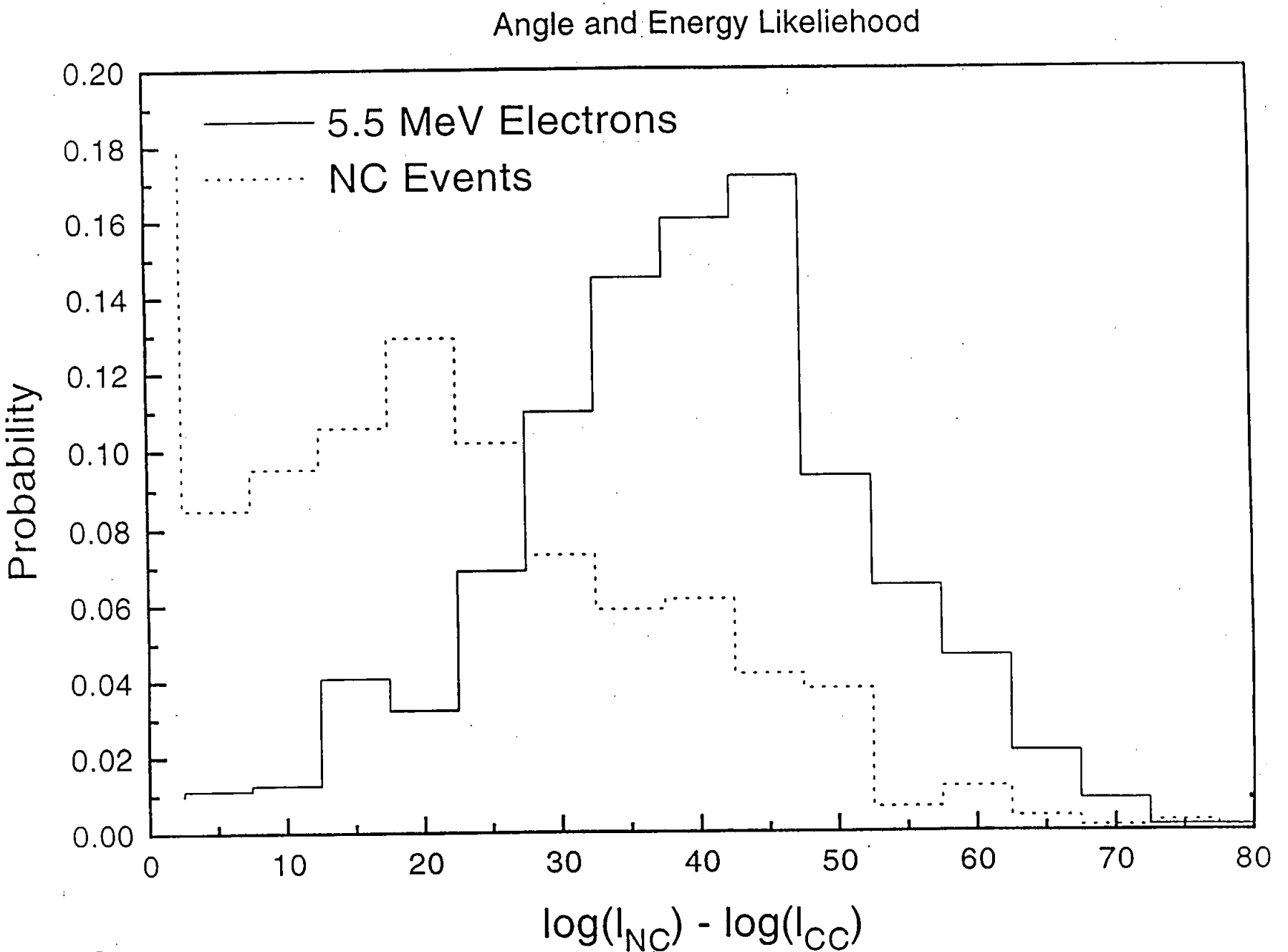
Angle and Energy Likeliehood
5.5 MeV Electrons
NC Events
Probability
0.20
0.18
0.16
0.14
0.12
0.10
0.08
0.06
0.04
0.02
0.00
0
10
20
30
40
50
60
70
80
log(l_NC) - log(l_CC)

Fig. 6

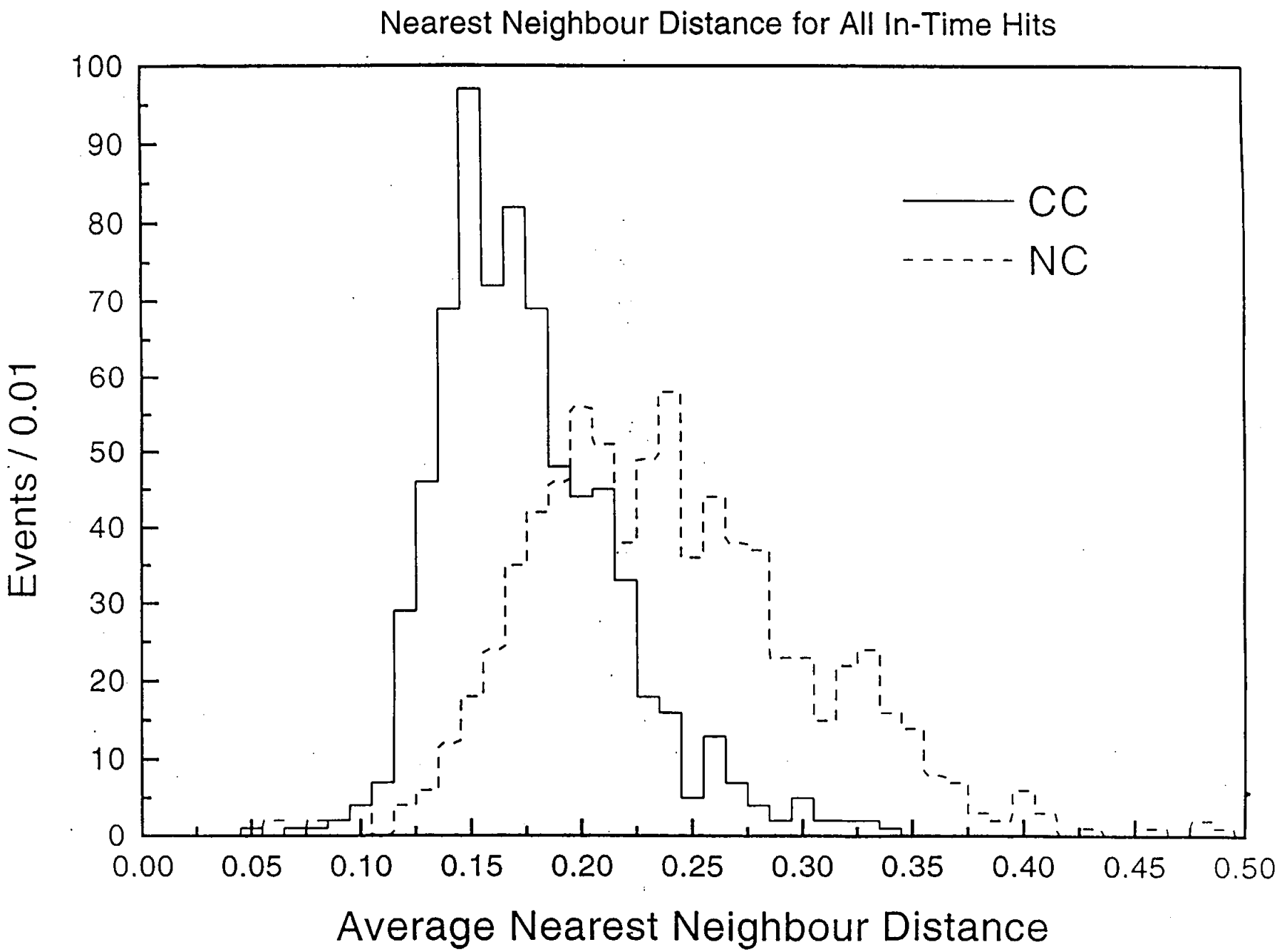
Nearest Neighbour Distance for All In-Time Hits
CC
NC
Events / 0.01
0
10
20
30
40
50
60
70
80
90
100
0.00
0.05
0.10
0.15
0.20
0.25
0.30
0.35
0.40
0.45
0.50
Average Nearest Neighbour Distance